Journal of Image Processing and Intelligent Remote Sensing
ISSN 2815-0953
Vol: 01, No. 02, Oct -Nov 2021
http://journal.hmjournals.com/index.php/JIPIRS
DOI: https://doi.org/10.55529/jipirs.12.8.16

A Dual-Transformer DC–DC with Variable Frequency Modulation Technique

P. Rajalakshmi*

**Department of EEE, Sri Chandrasekarendra Saraswathi viswa Maha Vidhyalaya, India*

*Corresponding Email: *p.rajalakshmi@kanchiuniv.ac.in*

Received: 08 July 2021 **Accepted:** 25 September 2021 **Published:** 18 October 2021

***Abstract:** For renewable power production systems to use less energy overall, power converters with improved efficiency over a wider load range are crucial. We introduce an unique dual-transformer DC-DC converter with many resonant components. With the right choice of resonance parameters, the converter can achieve a broad DC voltage gain range thanks to several resonance features. More resonance frequencies are included in the proposed converter as well, which will allow the load to receive more of the tertiary active power. Diodes achieve soft-switching or quasi-soft-switching during both the on and off periods, and all power switches are capable of on-soft switching. The proposed and analysis of variable frequency modulation (VFM) are achieved. By providing soft switching throughout the whole load range, the suggested modulation approach can lower switching losses. Additionally, the center-tapped bridge implementation of the synchronous rectifier further reduces conduction losses while the proposed modulation technique ensures soft switching of all devices. We installed a 500W prototype in the laboratory to confirm the theoretical analysis. According to the findings of the experiments, the suggested converter can maintain a relatively high efficiency (95%) throughout a wide load range. Starting with 300W, the highest efficiency is 95.4%.*

***Keywords:** Dual-Transformer DC–DC Converter, Variable Frequency Modulation, High Efficiency*

1. INTRODUCTION

The development of renewable energy and distributed energy storage systems has received a lot of attention lately due to the seriousness of the energy and environmental issues [1-2].One of the most crucial parts of this group is the home energy storage system. Technology advancements in the area of energy batteries have led to a rise in battery capacity, but the voltage used to charge the batteries has only slightly increased.

In general, non-isolated and isolated converters for bidirectional DC-DC converters are

Journal of Image Processing and Intelligent Remote Sensing
ISSN 2815-0953
Vol: 01, No. 02, Oct -Nov 2021
http://journal.hmjournals.com/index.php/JIPIRS
DOI: https://doi.org/10.55529/jipirs.12.8.16

distinguished [3]. This study only covers insulation converters because electrical insulation performance is a crucial safety assurance for residential energy storage systems [4]. One of the most fundamental isolation topologies is called DAB (Dual Active Bridge).

ZVS is lost, which further reduces efficiency, especially at light loads. Efficiency has been increased by the use of numerous enhanced topologies and control strategies [5]. The ZVS range is expanded in [6] by DAB using a SCI (Switch-Controlled-Inductor) resonant tank, and the greatest efficiency is 94.6 percent. On the other hand, if the gain is less than the rated amount, the efficiency will be drastically decreased and the output voltage range will be constrained. In order to increase effectiveness and eventually achieve 90%, we suggest control methods for the new prolonged phase shift in [7]. Unfortunately, even though these control measures are effective and sophisticated, more publicity is still needed.

Shakib and Mekhilef therefore suggested the variable frequency modulation (VFM) technique to address the issue of a greater voltage range (i.e., modifying the switching frequency to modulate the impedance of the LC tank). The suggested VFM [8] increases the voltage range while also assisting in soft switching. The harmonic content of harmonic currents, which could alter how accurately the estimated power is calculated, is not taken into account. persons on an equal footing. [9] regarded by the converter as harmonics. There is still a problem with high switching current during reflow and low power operation because of the single phase shift modulation, though. The two biggest obstacles to creating new modulation techniques are optimising harmonic effects and reducing losses.

Based on the fixed and variable switching frequencies of the suggested converter, this research investigates a new LC series resonant DAB and two new modulation approaches. The suggested modulation approach allows for the smooth rectifying of the switches on the primary and secondary sides of the HFT without the use of additional circuitry. As a result, without adding cost, modulation approaches can lower the converter's power loss across the full load range.

Consequently, the following list summarises the paper's significant contributions.

- A brand-new design for DC-DC converters with dual transmission is put forth. An output-side center-tapped bridge is cascaded through an LC series resonant tank- connected high-frequency transformer to create the input-side full-bridge converter.
- It has been created and tested to use VFM modulation techniques. By using the suggested modulation technique, the converter's capacity to transmit power is improved, allowing it to increase voltage gain while maintaining soft switching without the use of complex modulation or lossy components.

Proposed Converter

Journal of Image Processing and Intelligent Remote Sensing
ISSN 2815-0953
Vol: 01, No. 02, Oct -Nov 2021
http://journal.hmjournals.com/index.php/JIPIRS
DOI: https://doi.org/10.55529/jipirs.12.8.16

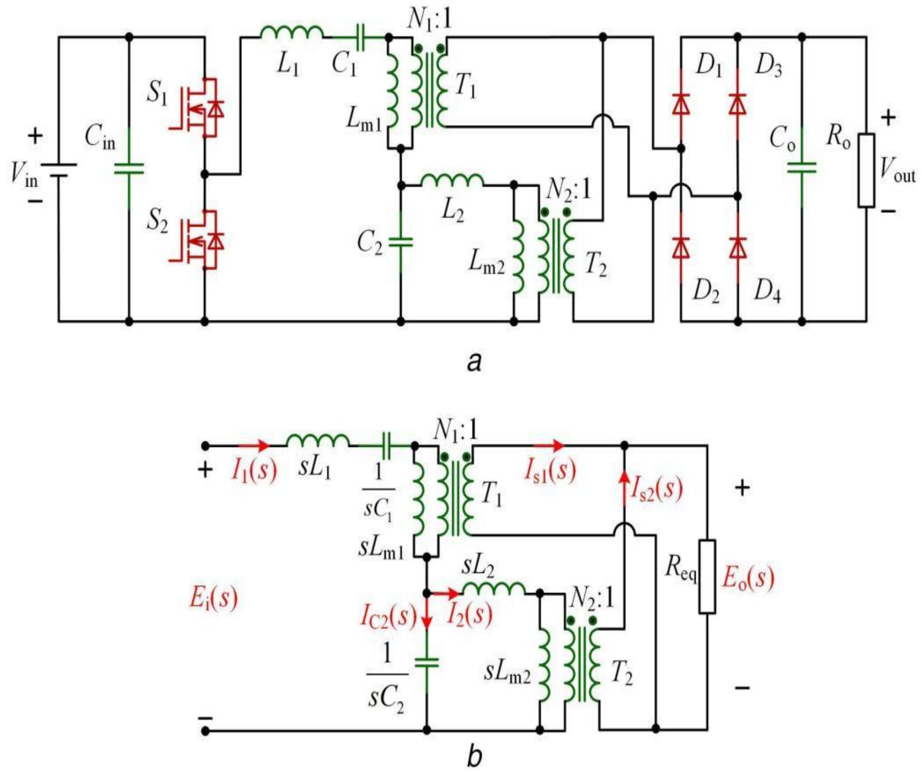

Figure 1: Proposed Dual Transformer DC-DC Converter

Various devices are shown in Figure 1 for a suggested two-transformer DC-DC resonant converter. Half-bridge inverter, resonant tank, and full-bridge diode rectifier are its three primary components. Inductors (L1, L2), capacitors (C1, C2), and high frequency transformers make up the resonant tank's six passive parts (T1, T2). Because of the multi- resonant architecture, the transducer can display a variety of resonant properties that set it apart from other LLC converters. Additionally, L1 and L2 are in series with the primary sides of T1 and T2, respectively, on the topological side. Connected to the midway of the rectifier is the secondary side that has been set up in parallel. Consequently, L1 and L2 absorb the respective leakage inductances of the two transformers. This significantly limits the negative effects of parasites on converter performance.

Simulation Setup:

Journal of Image Processing and Intelligent Remote Sensing
ISSN 2815-0953
Vol: 01, No. 02, Oct -Nov 2021
http://journal.hmjournals.com/index.php/JIPIRS
DOI: https://doi.org/10.55529/jipirs.12.8.16

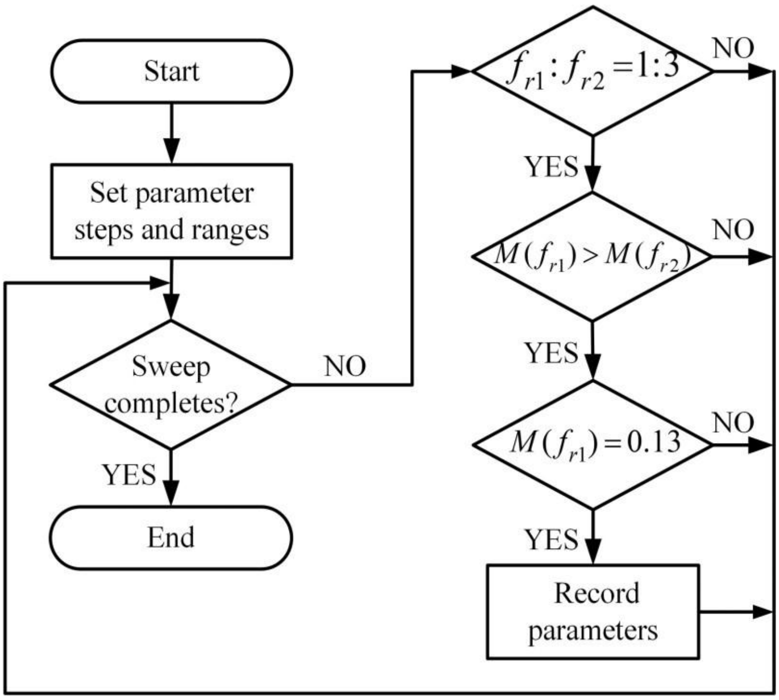

Figure 2: Flow Chart

The resonant capacitor's voltage stress is yet another crucial element that has a significant impact on the choice. The kind and cost of capacitors are directly impacted. The software receives 17 element packs in total according to the flowchart. Use PSIM software to simulate all of the component packages in order to compare voltage stress. It is possible to determine C1 and C2's respective peak voltages, VC1 and VC2, respectively. Figure 2 illustrates this representation of these voltages from highest to lowest based on the value of VC1. The selection range is also greater and the cost is lower the lower the voltage stress. Consequently, it is suggested to use short element packets of VC1 and VC2. The least amount of voltage stress is present in the 16th pack, as can be seen. The final planned MERC will be chosen as a result. The particular values are N1 = 2, N2 = 1.5, L1 = 190 µH, L2 = 25 µH, and C1 = C2 = 13nF. VC1 = 918V and VC2 = 452V, respectively, are the corresponding voltage stresses for C1 and C2.

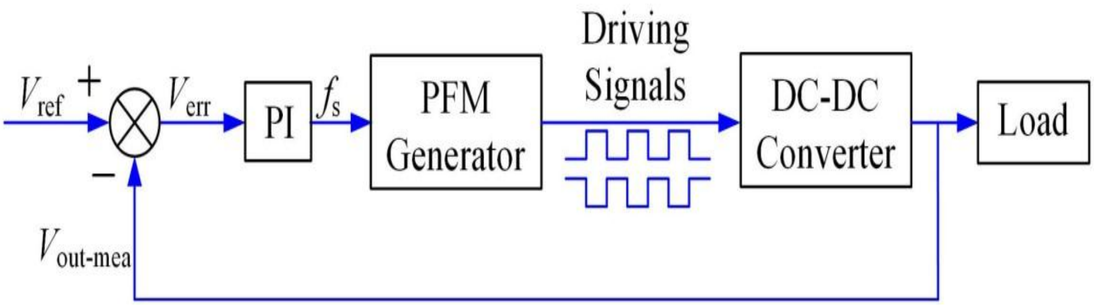

Figure 3: Block Diagram of the proposed method

Journal of Image Processing and Intelligent Remote Sensing
ISSN 2815-0953
Vol: 01, No. 02, Oct -Nov 2021
http://journal.hmjournals.com/index.php/JIPIRS
DOI: https://doi.org/10.55529/jipirs.12.8.16

For regulating the output voltage, this component employs a frequency modulation control approach. As seen in Figure 3, the control block diagram. As seen in the image, the proportional-integral (PI) controller receives the voltage error Verr between the constant reference voltage Vref and the output voltage that was measured. In order to create driving signals for all switches, the corrected result fs is next transmitted to a pulse frequency modulation generator.

2. EXPERIMENT RESULTS

To show the viability and effectiveness of the recommended topology and modulation, a 1.5kW LC-DAB prototype was constructed and tested (Figure 12). In the prototype, MOSFETs (IRPF4668, 200V) are used to construct a printed circuit board, and MOSFETs (IPW60R045CPA, 600V) are used to construct a synchronous rectifier. Each switch pair's dead time is configured to be 2 s. An FPGA creates the modulation, while the controller is programmed in a DSP (TMS320f28374d, 200MHz) (EPM570T100I, 66MHz). In order to reduce the impact of electromagnetic interference, the control board is placed on the opposite side of the heatsink.

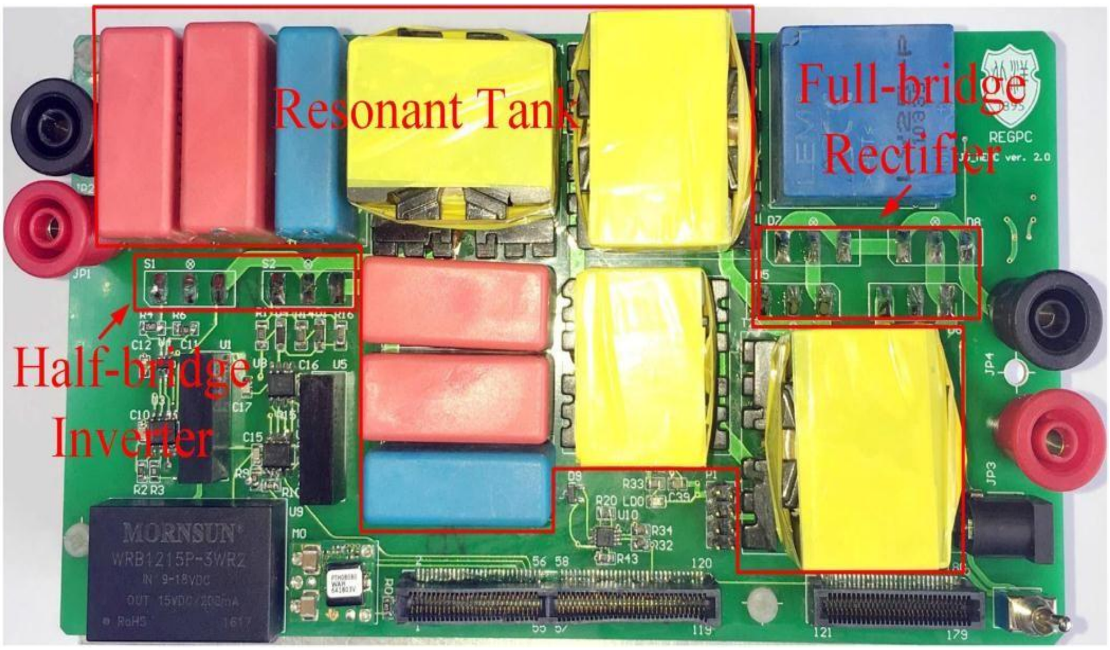

Figure 4: Proposed Prototype Model

The suggested converter's operating waveforms employing VFM at various operating locations are shown in Figure 4. Assuming that every gadget is perfect and devoid of parasites, simulations are carried out in MATLAB. The accuracy of theoretical waveforms, such as the computation of duty cycles and reverse current cutoff, can be demonstrated by simulation data.

Journal of Image Processing and Intelligent Remote Sensing
ISSN 2815-0953
Vol: 01, No. 02, Oct -Nov 2021
http://journal.hmjournals.com/index.php/JIPIRS
DOI: https://doi.org/10.55529/jipirs.12.8.16

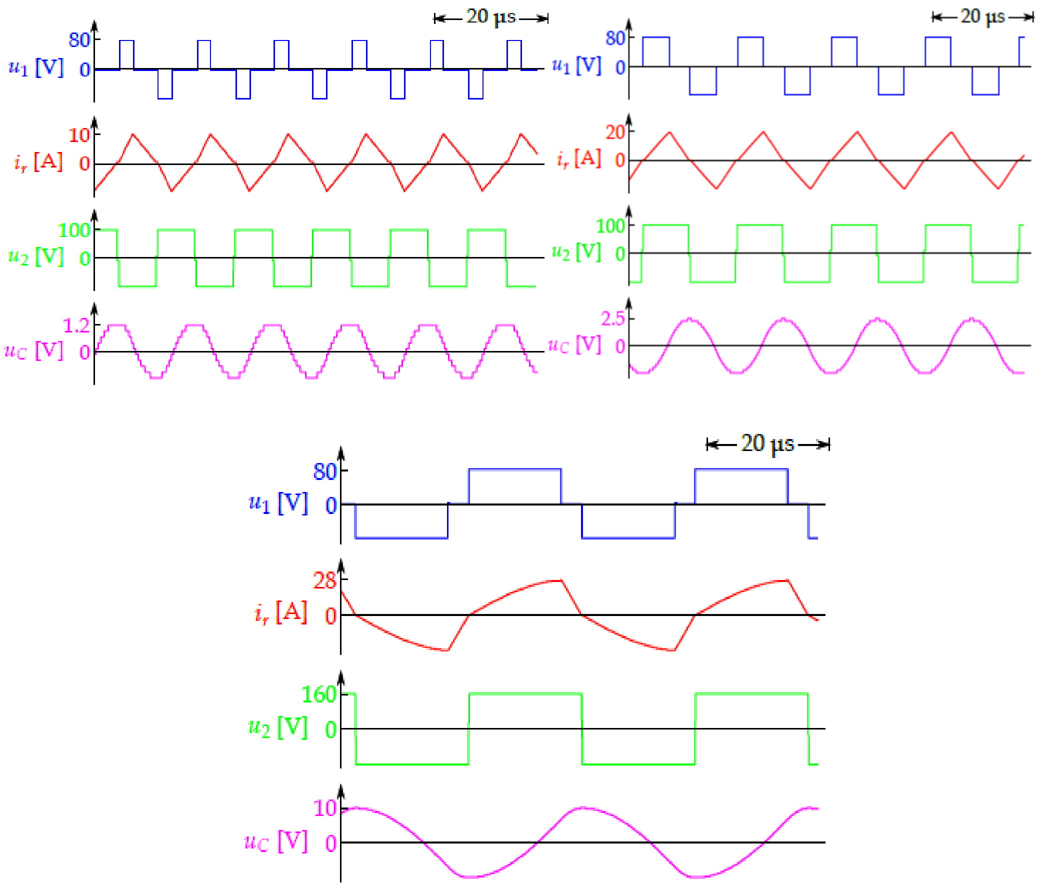

Figure 5**:** Experimental waveforms at different frequencies **(a)** 110 kHz, **(b)** 150 kHz, **(c)** 200 kHz

The prototype was put through its paces at 110kHz in Figure 5. In such a case, the third harmonic cannot be transmitted by the suggested transducer. The fundamental explanation for this is because the growth in 3fs happens considerably more quickly than the increase in fs. As a result, Mgain (3fs) is substantially different from Mgain, the comparable voltage gain (fr2). Since the input impedance exceeds Z3 by a wide margin, the third harmonic ratio of iS1 is almost zero. To achieve ZVS soft switching of all switches, the dual transformer MERC is still capable. By including iD1, it implements a quasi-ZCS turn-on switching function for diodes in addition to its own ZCS (Zero Current Switching) turn-off function.

Journal of Image Processing and Intelligent Remote Sensing
ISSN 2815-0953
Vol: 01, No. 02, Oct -Nov 2021
http://journal.hmjournals.com/index.php/JIPIRS
DOI: https://doi.org/10.55529/jipirs.12.8.16

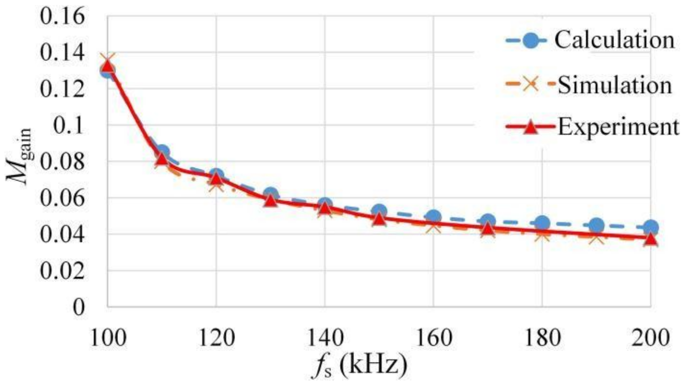

Figure 6: Comparison of the DC voltage gain curves

Comparative voltage gain curve analysis was done between the simulated, calculated, and experimental MERCs. Figure 1 displays the results. The three curves are perfectly aligned. However, if the operating frequency is distant from the rated frequency, the experimental results will vary slightly from the predicted results. This diagram illustrates how the suggested MERC modelling and design process works and how accurate it is.

At 300W, the converter's efficiency reaches a peak of 95,4%. At power levels greater than 200 W, it also retains high efficiency (~95%). Consequently, throughout a broad load range, great conversion efficiency can be ensured.

Two issues must be resolved in order to further increase conversion efficiency in the future. Synchronous rectifiers should be utilised, on the one hand. This strategy dramatically reduces the conduction losses of a diode because a MOSFET's on-resistance is much lower than that of a diode. Self-assembly methods are another option, but less likely.

3. CONCLUSION

In this study, a converter with VFM is suggested. The innovative two-transformers of MERC, we suggest and examine in this study. Inductors, capacitors, and high frequency transformers are all arranged in two pairs inside the resonant tank. The multiple resonance structure has given the MERC access to new resonance frequencies. Simulation and experimental results demonstrate the viability of topology and the modulation algorithm. The active power is carried by the first and third harmonics when the second frequency is set to be three times thefirst. The resonant current is therefore more efficiently utilised as a result. The suggested transducer also includes a voltage gain that may be varied over a broad range across a restricted frequency range. With almost any frequency deviance from the nominal point, the gain is altered from nominal to half value. As a last point, tests on a 500W prototype demonstrate that the suggested MERC achieves a high efficiency of 95% at power outputs above 200W. At 300W, the peak efficiency is 95.4%. It can decrease energy loss and enhance switchgear safety in the cases of solar power generation, electric vehicle charging, DC smart grid, etc.

Journal of Image Processing and Intelligent Remote Sensing
ISSN 2815-0953
Vol: 01, No. 02, Oct -Nov 2021
http://journal.hmjournals.com/index.php/JIPIRS
DOI: https://doi.org/10.55529/jipirs.12.8.16

4. REFERENCES

1. Lin, B.-R.: 'Modular resonant DC/DC converter for DC grid system applications',
2. IET Renew. Power Gener., 2017, 11, (7), pp. 952–958
3. Imran Shahzad, M., Iqbal, S., Taib, S.: 'A wide output range HB-2LLC resonant converter with hybrid rectifier for PEV battery charging', IEEE Trans. Transp.
4. Electrification, 2017, 3, (2), pp. 520–531
5. Gao, X., Wu, H., Xing, Y.: 'A multioutput LLC resonant converter with semiactive rectifiers', IEEE J. Emerging Sel. Topics Power Electron., 2017, 5, (4), pp. 1819– 1827
6. Malan, W.L., Mahinda Vilathgamuwa, D., Walker, G.R.: 'Modeling and control of a resonant dual active bridge with a tuned CLLC network', IEEE Trans. Power Electron., 2016, 31, (10), pp. 7297–7310
7. Zahid, Z.U., Dalala, Z.M., Chen, R., et al.: 'Design of bidirectional DC–DC resonant converter for vehicle-to-grid (V2G) applications', IEEE Trans. Transp.
8. Electrification, 2015, 1, (3), pp. 232–244
9. Chen, W., Rong, P., Lu, Z.: 'Snubberless bidirectional DC–DC converter with new CLLC resonant tank featuring minimized switching loss', IEEE Trans. Ind. Electron., 2010, 57, (9), pp. 3075–3086
10. Wu, H., Ding, S., Sun, K., et al.: 'Bidirectional soft–switching series-resonant converter with simple PWM control and load-independent voltage-gain characteristics for energy storage system in DC microgrids', IEEE J.Emerging Sel. Topics Power Electron., 2017, 5, (3), pp. 995–1007
11. Wu, X., Hu, C., Zhang, J., et al.: 'Analysis and design considerations of LLCC resonant multioutput DC/DC LED driver with charge balancing and exchanging of secondary series resonant capacitors', IEEE Trans. Power Electron., 2015, 30, (2), pp.780–789
12. Bommaraju, K., Manikandan, A., & Ramalingam, S. (2017). Aided System for Visually Impaired People in Bus Transport using Intel Galileo Gen-2: Technical Note. International Journal of Vehicle Structures and Systems, 9(2), 110–112. https://doi.org/10.4273/ijvss.9.2.09
13. Guan, Y., Wang, Y., Xu, D., et al.: 'A 1 MHz half-bridge resonant DC/DC converter based on GaN FETs and planar magnetics', IEEE Trans. Power Electron., 2017, 32, (4), pp. 2876–2891
14. Chen, J., Sha, D., Yan, Y., et al.: 'Cascaded high voltage conversion ratio bidirectional nonisolated DC–DC converter with variable switching frequency', IEEE Trans. Power Electron., 2018, 33, (2), pp. 1399–1409
15. Manikandan, A., & Pradeep, S. (2017). IoT Based Electricity Theft Detection. International Journal of Control Theory and Applications, 10(12), 211– 215.
16. Konjedic, T., Korosec, L., Truntic, M., et al.: 'DCM-based zero-voltage switching control of a bidirectional DC–DC converter with variable switching frequency', IEEE Trans. Power Electron., 2016, 31, (4), pp. 3273–3288.
17. Sun, J.; Sun, Q.; Ma, D.; Wang, P. Improved dynamic response strategy with dual phase-shift control for dual-active-bridge DC–DC converter. IET Power Electron. 2020, 13, 2671–2674.

Journal of Image Processing and Intelligent Remote Sensing
ISSN 2815-0953
Vol: 01, No. 02, Oct -Nov 2021
http://journal.hmjournals.com/index.php/JIPIRS
DOI: https://doi.org/10.55529/jipirs.12.8.16

18. Guan, M. A Series-Connected OffshoreWind Farm Based on Modular Dual-Active-Bridge (DAB) Isolated DC–DC Converter. IEEE Trans. Energy Convers. 2019, 34, 1422–1431.
19. Leo, S.; Jean-Paul, F.; David, F.; Pierre-Olivier, J.; Pierre, P.; Othman, L. Implementation of monolithic bidirectional switches in a AC/DC Dual Active Bridge in ZVS auto-switching mode. In Proceedings of the 2018 IEEE International Conference on Industrial Technology (ICIT), Lyon, France, 20–22 February 2018; pp.742–746.
20. Wang, M.; Guo, S.; Huang, Q.; Yu, W.; Huang, A.Q. An Isolated Bidirectional Single-Stage DC-AC Converter Using Wide-Band-Gap Devices With a Novel Carrier-Based Unipolar Modulation Technique Under Synchronous Rectification. IEEE Trans. Power Electron. 2017, 32, 1832–1843.
21. Sun, X.; Shen, Y.; Li, W.; Wang, B.; Wang, L.; Li, X. Center-tapped transformer based bidirectional dc-dc converter with wide input voltage range. In Proceedings of the 2015 IEEE Energy Conversion Congress and Exposition (ECCE), Montreal, QC, Canada, 20–24 September 2015; pp. 5910–5917.
22. Manikandan, A., & Nirmala, V. (2015). A Low Cost Thermoelectric Refrigerator. International Journal of Applied Engineering Research, 10(55), 3097– 3101.
23. Pant, B.; Kundu, U.; Sensarma, P. Analysis of series and parallel tank for dual active bridge single phase inverter application. In Proceedings of the 2017 National Power Electronics Conference (NPEC), Pune, India, 18–20 December 2017; pp. 258–263